Supplementary Information for:

Springtime Nitrogen Oxide-Influenced Chlorine Chemistry in the Coastal Arctic

Stephen M. McNamara[1], Angela R. W. Raso[1,2$], Siyuan Wang[1†], Sham Thanekar[3], Eric Boone[1,2], Katheryn R. Kolesar[1◊], Peter K. Peterson[1#], William R. Simpson[4], Jose D. Fuentes[3], Paul B. Shepson[2,5‡], Kerri A. Pratt[1,6*]

[1]Department of Chemistry, University of Michigan, Ann Arbor, MI, USA
[2]Department of Chemistry, Purdue University, West Lafayette, IN, USA
[3]Department of Meteorology, Pennsylvania State University, University Park, PA, USA
[4]Department of Chemistry and Biochemistry, University of Alaska Fairbanks, Fairbanks, AK, USA
[5]Department of Earth, Atmospheric, and Planetary Sciences & Purdue Climate Change Research Center, Purdue University, West Lafayette, IN, USA
[6]Department of Earth and Environmental Sciences, University of Michigan, Ann Arbor, MI, USA
[$]Now at the New Mexico Environment Department, Santa Fe, NM, USA
[†]Now at the National Center for Atmospheric Research, Boulder, CO, USA
[◊]Now at Air Sciences Inc., Portland, OR, USA
[#]Now at the Department of Chemistry, Whittier College, Whittier, CA, USA
[‡]Now at the School of Marine & Atmospheric Sciences, Stony Brook University, Stony Brook, NY, USA

*Corresponding Author: Kerri A. Pratt
Department of Chemistry, University of Michigan
930 N. University Ave.
Ann Arbor, MI 48109
prattka@umich.edu
(734) 763-2871

Summary (24 pages with 1 table, 2 text sections, and 13 figures)

- **Table S1**: Overview of CIMS, O_3, and NO_x measurements and figures of merit.
- **Figure S1**: CIMS reagent ion signal during ambient sampling.
- **Figure S2**: Isotopic ratio plots for Cl_2, $ClNO_2$, ClO, and BrCl (10 min averaged) for all days and polluted-only days.
- **Figure S3**: Representative mass spectra for Cl_2, HO_2NO_2, $ClNO_2$, N_2O_5, and BrCl.
- **Figure S4**: Performance of the CIMS glass wool background scrubber.
- **Figure S5**: Comparison of the N_2O_5 mass scan and selected ion monitoring data.
- **Section S2**: Identification of halogen species using isotopic ratios.
- **Section S3**: Offline calibration procedures for $ClNO_2$, N_2O_5, ClO, BrCl, HO_2NO_2, and HNO_3.
- **Figure S6**: NO and NO_2 wind rose plots, and description of sampling sites.
- **Figure S7**: Representative HYSPLIT backward air mass trajectories and measurements of wind speed/direction to show influence from the North Slope of Alaska oilfields.
- **Figure S8**: Trace gas observations during the three polluted periods.
- **Figure S9**: Observations of relationship between Cl_2 and O_3.
- **Figure S10**: Cl_2 mole ratios vs. NO mole ratios.
- **Figure S11**: Vertical potential temperature measurements from daily soundings at Utqiaġvik.
- **Figure S12**: HNO_3 measurements from April 8-May 20, 2016.
- **Figure S13**: $ClNO_2$ and N_2O_5 mole ratios, air temperature, and solar radiation measurements during the three polluted periods.

S1. Chemical ionization mass spectrometer (CIMS) operation

Table S1: Overview of CIMS, O_3, and NO_x measurements and figures of merit

CIMS-Specific Parameters

Species	Ions Quantified (m/z)[a]	3σ LOD (ppt)	3σ LOD 10 min avg. (ppt)	Measurement Uncertainty % + LOD, (ppt)	In-field Sensitivity (Hz ppt^{-1})[b]	Relative Sensitivity (to Cl_2 or Br_2)
ClO	$I^{35}ClO^-$ *m/z* 178	2	1	47% + 2		0.3 ± 0.1[c]
HNO_3 (after Apr 8)[f]	$IHNO_3^-$ *m/z* 190	19	10	30% + 19		3.8 ± 0.9[d]
Cl_2	$I^{35}Cl^{37}Cl^-$ *m/z* 199	0.8	0.5	22% + 0.8	14 – 22	
HO_2NO_2	$IHO_2NO_2^-$ *m/z* 206	15	8	30% + 15		0.025 ± 0.001[e]
$ClNO_2$	$I^{35}ClNO_2^-$ *m/z* 208	0.3	0.2	22% + 0.3		5.6 ± 0.6[d]
N_2O_5 (after May 8)[g]	$IN_2O_5^-$ *m/z* 235	1	0.8	24% + 1		1.3 ± 0.1[d]
BrCl	$I^{81}Br^{35}Cl^-$ and $I^{79}Br^{37}Cl^-$ *m/z* 243	3	2	39% + 3		1.6 ± 0.5[d]
Br_2	$I^{79}Br^{81}Br^-$ *m/z* 287	1	0.8	29% + 1	36 – 67	

Additional Measurements

Species	Instrument	LOD	Dates available
O_3	2B Instruments, Model 205	1 ppb	Mar 4 – May 20
NO	Thermo Scientific, Model 42i	0.4 ppb	Mar 11-20, Mar 25-Apr 2, May 11-19
NO_2	MAX-DOAS[ref 1–3]	2.5 x 10^{15} molec. cm^{-2}	Mar 4 – May 20

[a]All dwell times were 500 ms except for $IHNO_3^-$ at *m/z* 190, which was 200 ms.
[b]Range is mean ± calculated uncertainty for the campaign.
[c]Relative to Cl_2 (*m/z* 197). [d]Relative to Cl_2 (*m/z* 199). [e]Relative to Br_2 (*m/z* 287).
[f]Due to high instrument backgrounds, only HNO_3 data from after Apr 8 are presented (**Figure S12**)
[g]For N_2O_5 quantified by hourly mass scans (Mar 4 – May 8), the LOD was estimated as 12 ppt.

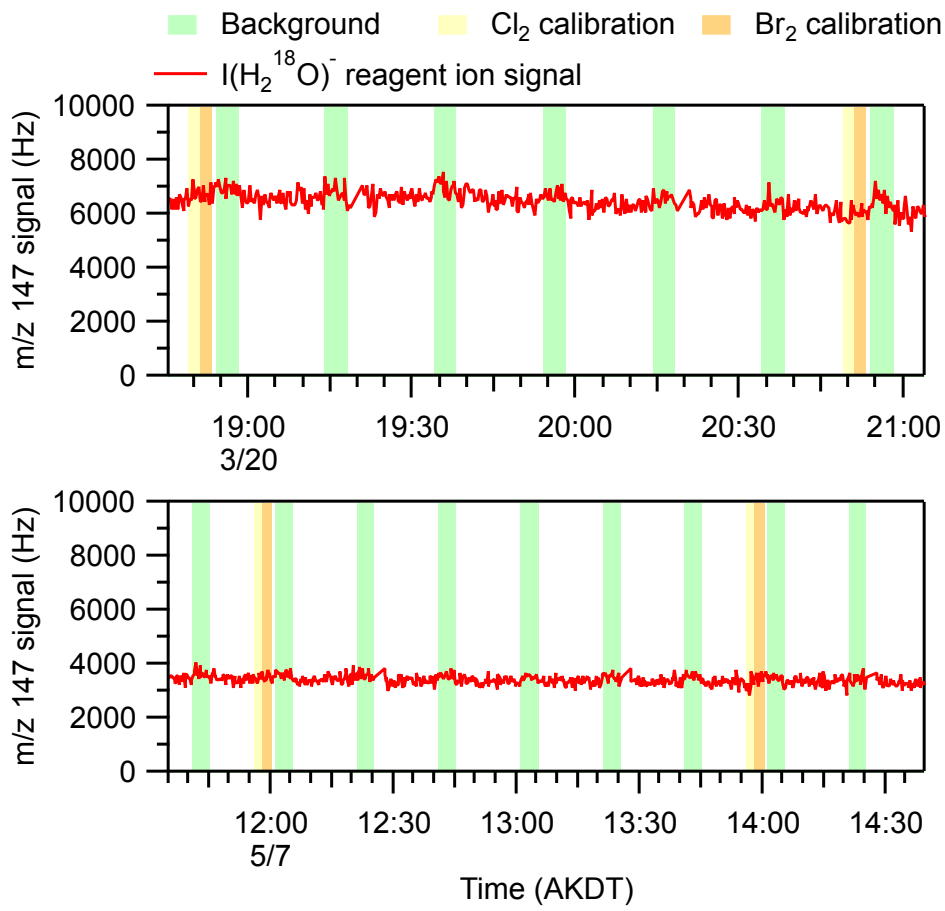

62

63 **Figure S1:** Reagent ion signal, monitored at *m/z* 147 as $I(H_2{}^{18}O)^-$, during ambient sampling,

64 backgrounds, and calibrations at two example periods during the campaign.

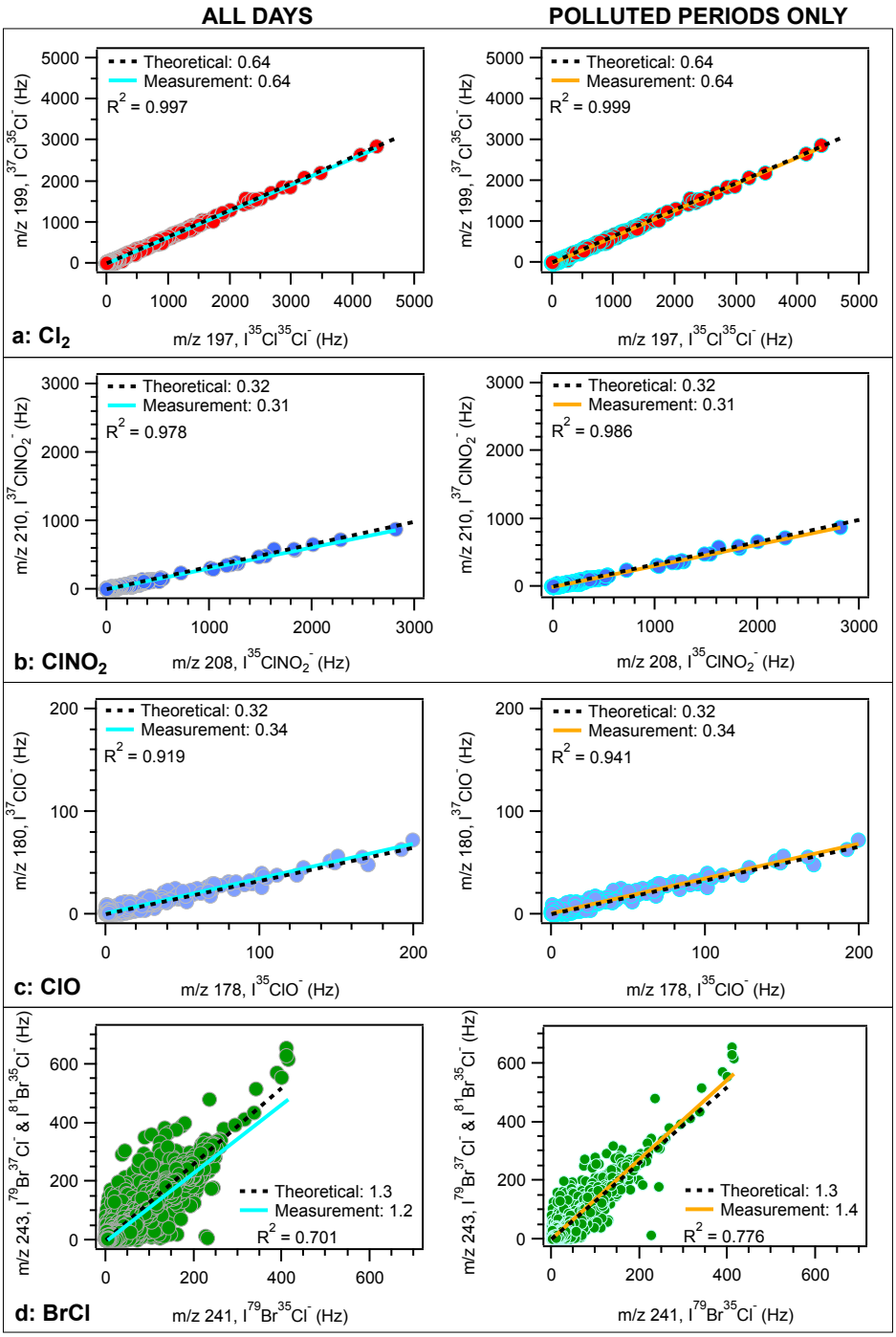

Figure S2: 10 min averaged measured signals (background subtracted) of (**A**) *m/z* 199 vs *m/z* 197, (**B**) *m/z* 210 vs *m/z* 208, (**C**) *m/z* 180 vs *m/z* 178, and (**D**) *m/z* 243 vs *m/z* 241 showing isotopic ratios used to identify Cl_2, $ClNO_2$, ClO, and BrCl, respectively, from March 4 – May 20, 2016 (*left column*) and during the three polluted periods only (*right column*). The black dashed lines are the

theoretical isotopic ratios and the solid lines are the measured ratios. For ClO in (C), all data observed to be impacted by a mass interference at *m/z* 180 are not included here.

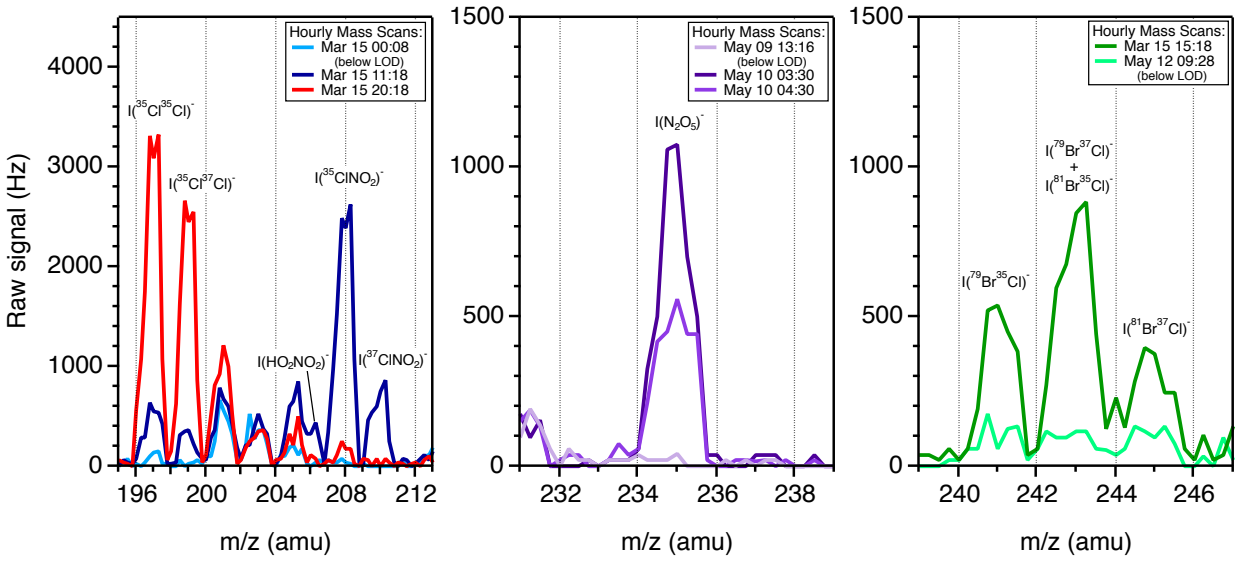

72

73 **Figure S3:** Representative mass spectra (at *m/z* 195-213, *m/z* 231-239, and *m/z* 239-247)
74 comparing when Cl_2, HO_2NO_2, $ClNO_2$, N_2O_5, and BrCl were abundant versus times when signals
75 were below detection limits (noted as "(below LOD)" in plot legends). All mass scans used a 0.25
76 amu step size and 100 ms dwell time.

77

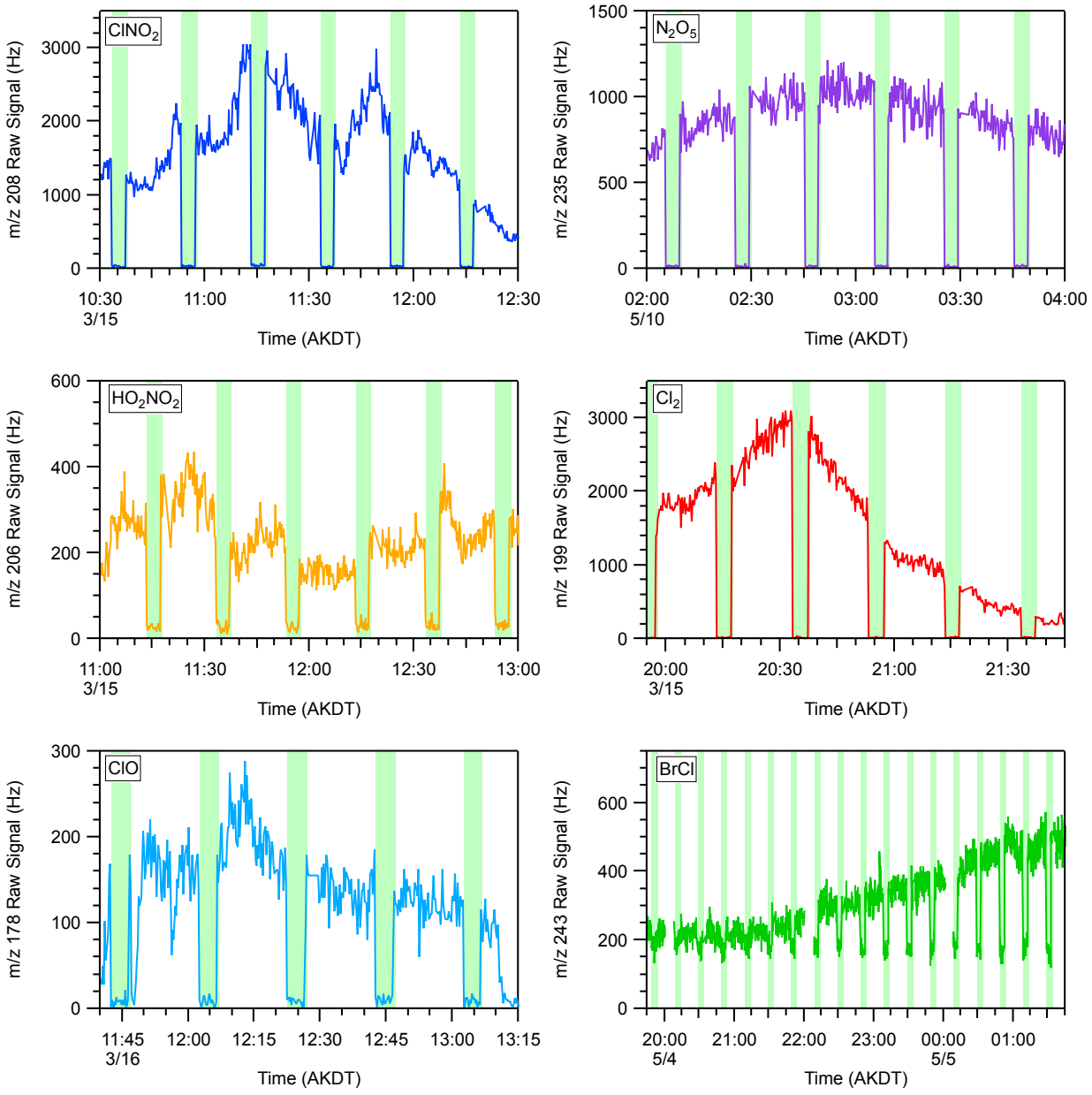

78

79 **Figure S4:** Performance of the glass wool scrubber during high-abundance periods of $ClNO_2$,
80 N_2O_5, HO_2NO_2, Cl_2, ClO, and BrCl, with background periods shown by green shading. A constant
81 interference was present from *m/z* 241 – *m/z* 245 that was not removed by the scrubber, leading to
82 the elevated signal during backgrounds for BrCl. However, these background signals were not

consistent with BrCl isotopic ratios and therefore did not impact the scrubber's ability to remove BrCl.

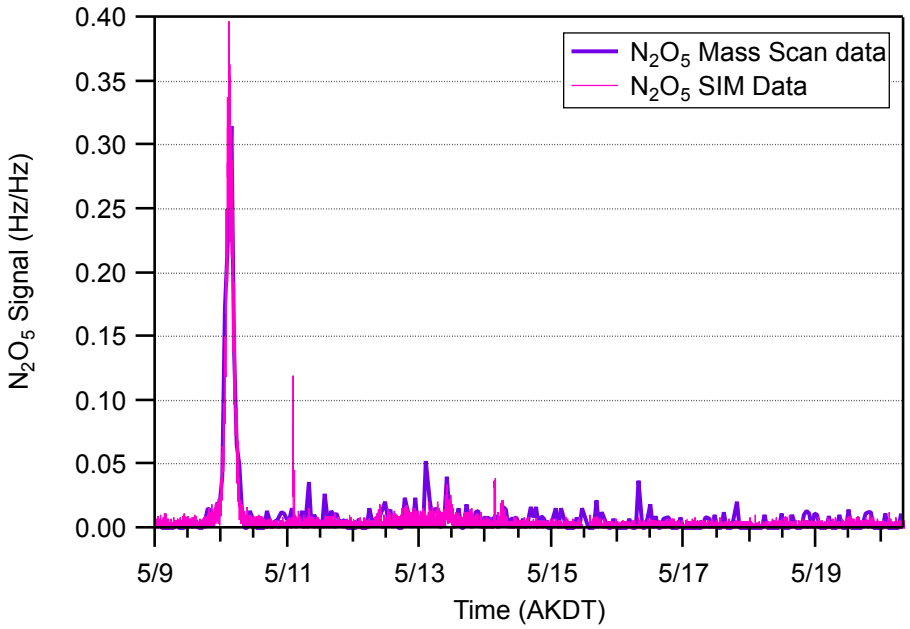

Figure S5: Comparison of N_2O_5 mass scan and selected ion monitoring (SIM) data, during the period of overlap from May 9-20, 2016. The estimated N_2O_5 mass scan LOD of 12 ppt was estimated using the SIM background period (4 min, LOD = 1 ppt), while accounting for the shortened mass scan dwell time (100 ms). Since the signal variation is assumed to be dominated by counting statistics,[4] we account for the difference in dwell times by taking the square root of this factor (the 100 ms mass scan is a factor of 80 shorter than the total dwell time during the 4 minute SIM background period) to estimate the mass scan LOD.

S2. Identification of halogen species using isotopic ratios

The measured isotopic ratios of the halogen species were used to confirm their identities. Signals of two isotopes for the same species (e.g., $I^{35}Cl^{37}Cl^-$ vs. $I^{35}Cl^{35}Cl^-$ for Cl_2), averaged to 10 minutes, were plotted against each other and the slope of a linear regression was compared to the theoretical isotopic ratio (**Figure S2**). We report the following measured ratios, in comparison to the theoretical ratios, for all days of the campaign: For *m/z* 199 vs *m/z* 197, the measured ratio of 0.64 (R^2 = 0.997) confirmed the identity of Cl_2 (theoretical = 0.64). For *m/z* 210 vs *m/z* 208, the measured ratio of 0.31 (R^2 = 0.978) confirmed the identity of $ClNO_2$ (theoretical = 0.32). For *m/z* 180 vs *m/z* 178, the measured ratio of 0.34 (R^2 = 0.919) confirmed the identity of ClO (theoretical = 0.32). A mass interference at *m/z* 180 ($I^{37}ClO^-$) was observed, which resulted in ClO not being quantifiable from March 25 – April 30, when the ratio of *m/z* 180 to *m/z* 178 ($I^{35}ClO^-$) varied by >30%. For *m/z* 243 vs *m/z* 241, the measured ratio of 1.2 (R^2 = 0.701) confirmed the identity of BrCl (theoretical = 1.3).

S3. Offline calibrations of $ClNO_2$, N_2O_5, ClO, BrCl, HO_2NO_2, and HNO_3

S3.1. $ClNO_2$

Nitryl chloride ($ClNO_2$) was calibrated using a modified procedure of *Thaler et al.*[5] In the laboratory, $ClNO_2$ was synthesized by passing 0 – 50 ppb Cl_2 over a 1.0 mL bed of 0.01 M $NaNO_2$ solution. The synthesized $ClNO_2$ was then passed through a 300°C quartz tube oven, where it was completely thermally dissociated (complete loss of $ClNO_2$ signal at *m/z* 208 and 210). The resulting NO_2 was quantified using a custom NO_x analyzer[6] equipped with a blue light-emitting diode to photochemically reduce NO_2 to NO for measurement.[7] The $ClNO_2$ sensitivity (at *m/z* 208) relative to Cl_2 (at *m/z* 199) was determined to be 5.6 ± 0.6.

S3.2. N_2O_5

Dinitrogen pentoxide (N_2O_5) was calibrated using a modified procedure of *Bertram et al.*[8] N_2O_5 was synthesized by combining flows of NO_2 and O_3 in a 61 cm long, 2.2 cm diameter PFA tube with a 1.5 min residence time (flow rate of 2.7 cm^3 s^{-1}). N_2O_5 was quantified using the custom NO_x analyzer described in Section S3.1[6,7] by measuring the amount of NO_2 reacted upon the addition of O_3, assuming two moles of NO_2 are reacted to form one mole of N_2O_5 (R7-R8). Loss of NO_2 due to excess NO_3 formation was negligible. For NO_2 at 40 ppb within the PFA tube during the calibration, the $[NO_3]$ / $[N_2O_5]$ ratio was calculated to be 0.04. The N_2O_5 sensitivity (at *m/z* 235) relative to Cl_2 (at *m/z* 199) was determined to be 1.3 ± 0.1.

S3.3. ClO

The relative sensitivity of 0.3 ± 0.1 for chlorine monoxide (ClO) (*m/z* 178) / Cl_2 (*m/z* 197) determined by *Custard et al.*[9] was applied for the ambient measurements for this study. For this calibration, ClO was synthesized in a quartz flow tube via the photolysis of Cl_2 with excess O_3 (90

ppb) and ~5 ppb of NO_2.[9] The steady-state ClO concentration was determined using the measured photolysis rate of Cl_2 and measurements of Cl_2 and NO_2 mole ratios.[9]

S3.4. BrCl

Bromine chloride (BrCl) was synthesized by passing Cl_2 over a 1 mL bed of 1 M NaBr solution in a glass reaction vessel, similar to *Huff et al.*[10] The output of the reaction vessel was predominately BrCl, Br_2, and the remaining Cl_2, as measured by CIMS. It is likely the observed Br_2 was a product of a subsequent reaction of BrCl and bromide (Br^-).[10] The reaction output was bubbled into 10 mL of sodium bicarbonate/sodium metabisulfite buffer solution in a glass impinger for 40 min, allowing the following reactions with the molecular halogens to occur (RS1 –RS3, where X = Cl or Br):

$$X_{2(g)} + 2OH^-_{(aq)} \rightarrow X^-_{(aq)} + OX^-_{(aq)} + H_2O \quad \text{(RS1)}$$

$$OX^-_{(aq)} + HSO_3^-{}_{(aq)} \rightarrow X^-_{(aq)} + SO_4^{2-}{}_{(aq)} + H^+_{(aq)} \quad \text{(RS2)}$$

$$\textbf{Net: } X_{2(g)} + 2OH^-_{(aq)} + HSO_3^-{}_{(aq)} \rightarrow 2X^-_{(aq)} + SO_4^{2-}{}_{(aq)} + H^+_{(aq)} \quad \text{(RS3)}$$

The total chloride concentration of the buffer solution following bubbling of the reaction output was measured using a Dionex ICS-2100 ion chromatograph. A blank solution (N_2 bubbled only) was also collected as a background measurement, and the background Cl^- (accounting for ~4-10%) was subtracted from the total measured Cl^- in the reaction output solution. Following the background subtraction, the Cl^- resulting from the remaining Cl_2 was subtracted from the total measured Cl^- using the Cl_2 signal measured by CIMS in parallel. The BrCl was then quantified as the remaining chloride in the solution following subtraction of the chloride from unreacted Cl_2 and the blank (background Cl^-). The headspace of the impinger during the bubbling period was monitored with CIMS, and no Cl_2, BrCl, or Br_2 was observed; therefore, the output of the reaction

vessel was sufficiently captured by the buffer solution. The resulting BrCl sensitivity (at *m/z* 243) relative to Cl_2 (at *m/z* 199) was determined to be 1.6 ± 0.5.

S3.5. HO_2NO_2

Peroxynitric acid (HO_2NO_2) was synthesized following *Appelman and Gosztola*[11] and was obtained in the gas-phase by bubbling N_2 through an impinger containing the synthesized peroxynitric acid in a solution of hydrogen peroxide on ice. The HO_2NO_2 was quantified using the NO_2 generated from its thermal decomposition at 140°C within a 91 cm Teflon tube, and it was assumed that the thermal decomposition of each HO_2NO_2 molecule led to the formation of one NO_2 molecule. The NO_2 was monitored using a custom chemiluminescence NO_y instrument, constructed following previous methods[12–14] and calibrated using a NO_2 standard cylinder (Praxair).

S3.6. HNO_3

Nitric acid (HNO_3) was calibrated in the laboratory by adding to the CIMS inlet flow 0.2 L min^{-1} of HNO_3 (in N_2) from a 50 ng min^{-1} HNO_3 permeation source (VICI Metronics, Inc.). The HNO_3 mole ratio was varied from 0.8 – 9.7 ppb to obtain a calibration curve. The HNO_3 permeation rate was confirmed by bubbling the HNO_3 flow into 4 mL of micropure water, and the resulting nitrate concentration was quantified using a Dionex ICS-2100 ion chromatograph. The HNO_3 sensitivity (at *m/z* 190, $IHNO_3^-$) relative to Cl_2 (at *m/z* 199) was determined to be 3.8 ± 0.9.

S4. Additional data figures

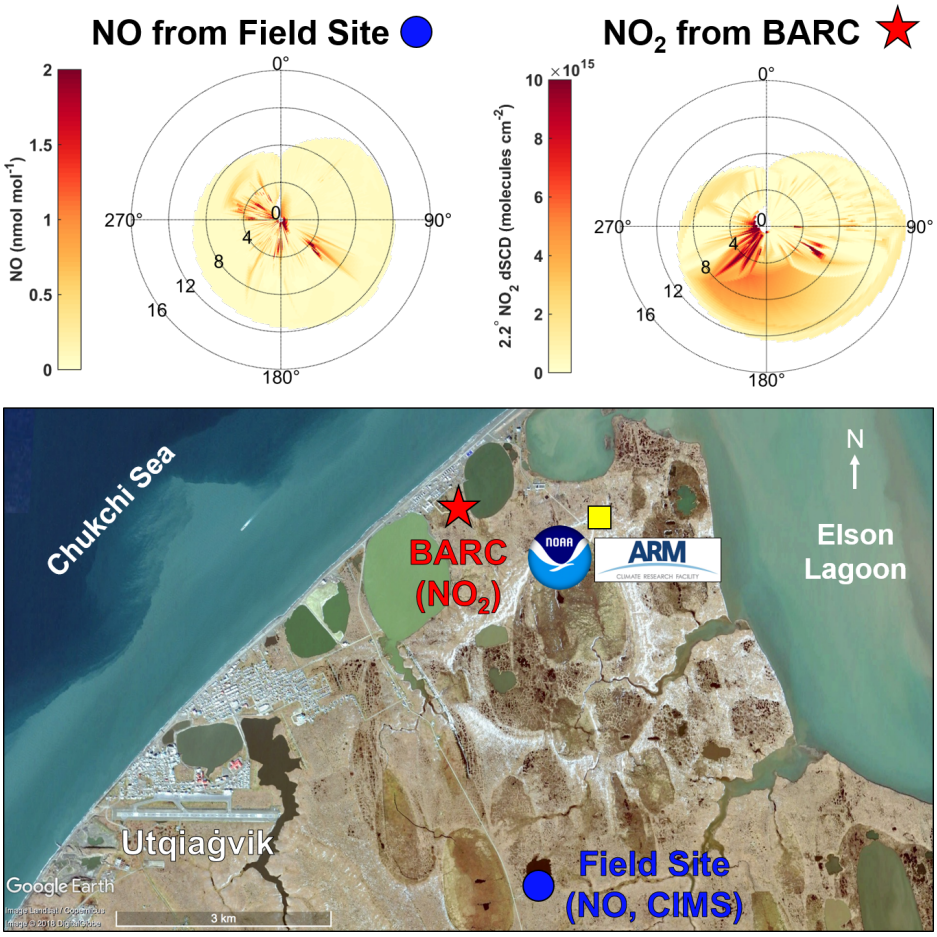

Figure S6: Wind rose plots, colored by NO mole ratios (*top-left*) and NO_2 differential slant column densities (dSCDs, *top-right*) and a map of the region (*bottom*). *In situ* NO was measured at the main field site (blue circle), located ~5 km ESE of Utqiaġvik, and NO_2 measured from the Barrow Arctic Research Center (BARC, red star), ~5 km NW of Utqiaġvik. From March 4 – 17, wind direction (°) and wind speeds (m s^{-1}) measured at the NOAA Barrow Observatory (yellow square), with wind measurements occurring at the main field site for the remainder of the study. The ARM Research Facility is located next to the NOAA Observatory (yellow square).

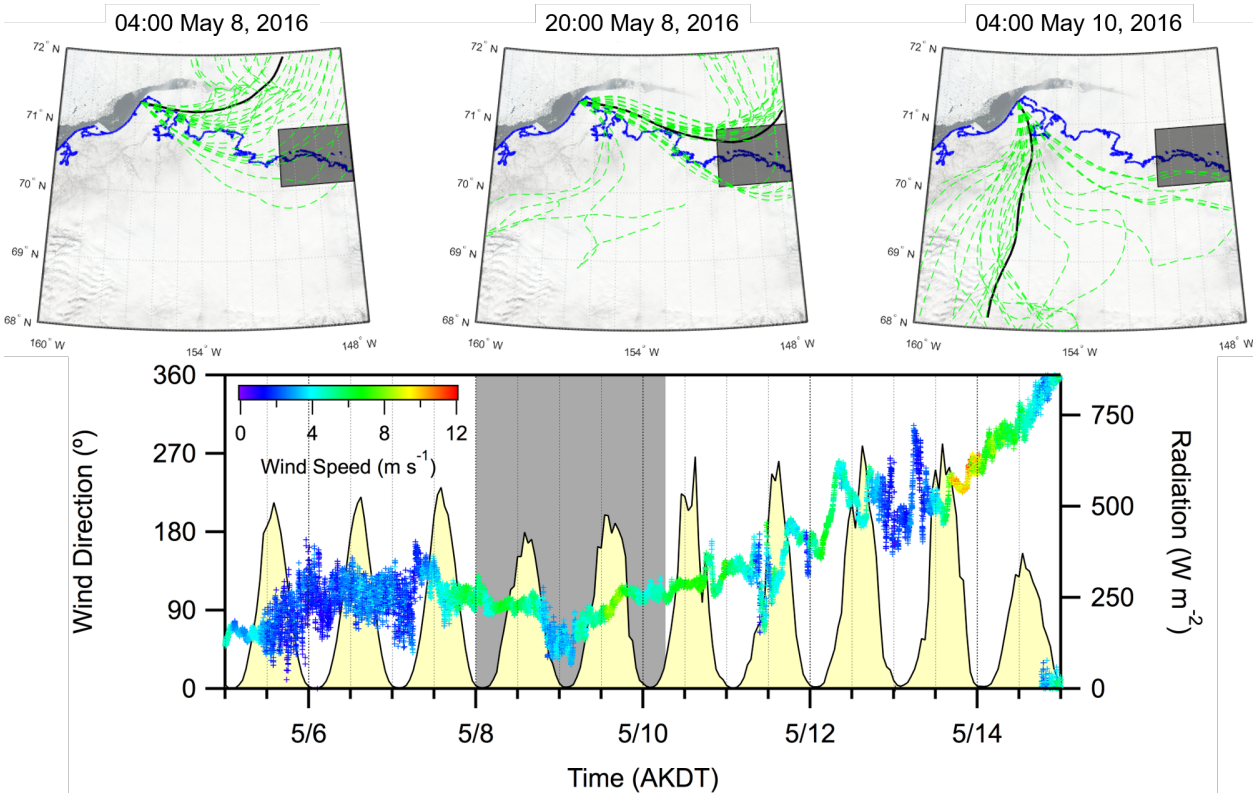

Figure S7: (*top panels*) Representative HYSPLIT 72-hour backward air mass trajectories (black lines) arriving at Utqiaġvik at 04:00 AKDT May 8 (*left*), 20:00 AKDT May 8 (*middle*), and 04:00 AKDT May 10 (*right*). Green dashed lines are ensemble members of the trajectories, which represent uncertainty. Portions of the trajectories and ensemble members travel through the gray-shaded region representing the North Slope of Alaska and Prudhoe Bay Oilfields.[15] For reference, the full period of "Prudhoe Bay Influence", defined as times when air mass trajectories traveled through the gray-shaded region, was determined to be 00:00 AKDT May 8 to 05:00 AKDT May 10. (*lower panel*) Wind direction, wind speed, and solar radiation observations from May 5 – 15, 2016, with the gray shading representing the Prudhoe Bay-influenced period determined from the HYSPLIT trajectories.

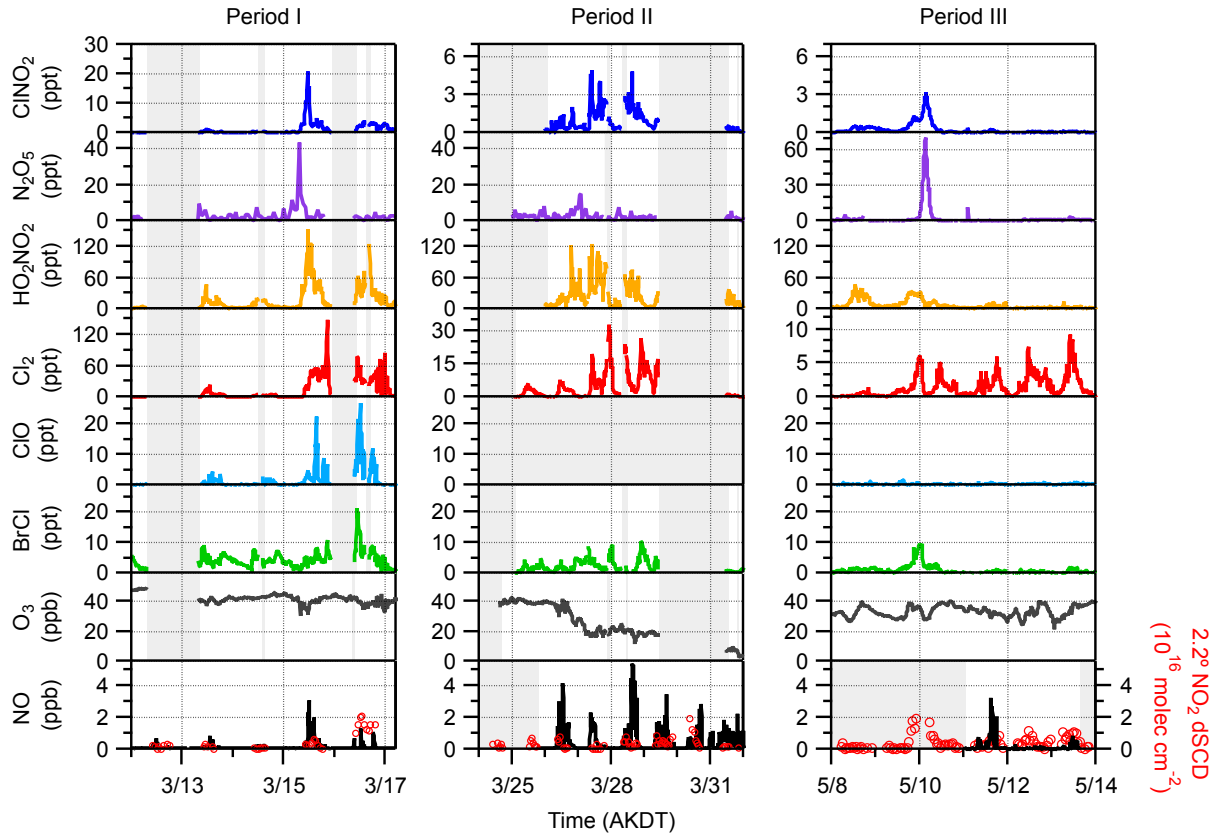

190

191 **Figure S8:** Observations of $ClNO_2$, N_2O_5, HO_2NO_2, Cl_2, ClO, BrCl, O_3, NO, and NO_2 during the
192 three episodes of enhanced chlorine chemistry (March 12-16, March 24-31, and May 8-13, 2016)
193 near Utqiaġvik, AK. Gray shading denotes periods without CIMS, O_3, or NO data available due to
194 site power loss and use for other experiments. During Period II, ClO could not be quantified due
195 to a mass interference.

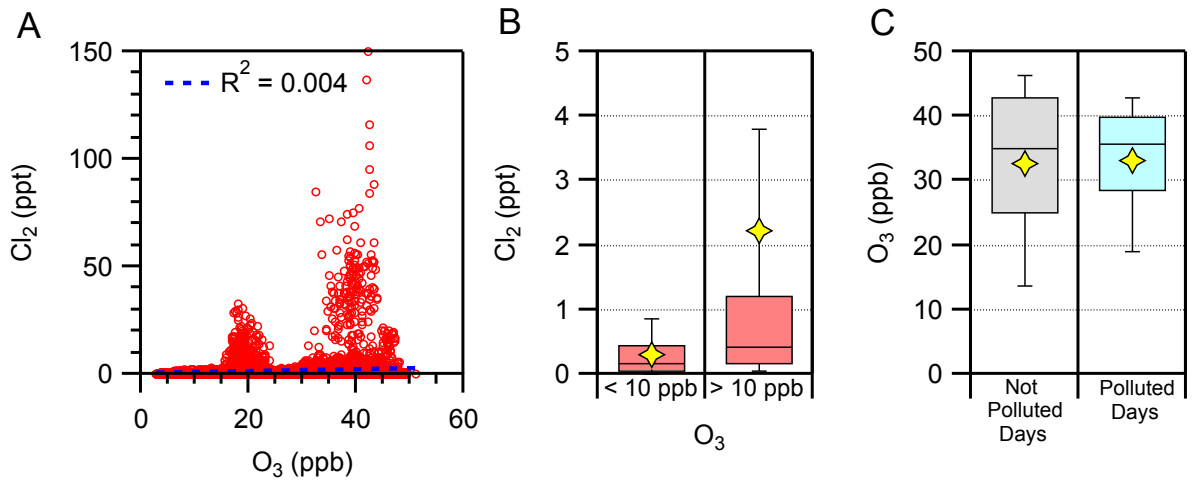

196

197 **Figure S9:** (**A**) Cl_2 mole ratios vs O_3 mole ratios (10 min averaged). Box and whisker plots show
198 the distributions (90th/10th and 75th/25th percentiles, and medians) of (**B**) Cl_2 mole ratios, binned
199 by O_3 mole ratios less or greater than 10 ppb, and (**C**) O_3 mole ratios, binned by Not Polluted and
200 Polluted days (defined in Section 2.2 and used in Figure 2B). Yellow stars represent average mole
201 ratios for the given populations. Elevated Cl_2 was observed when O_3 was near background levels
202 (typically > 20 ppb), and Cl_2 was near zero when O_3 was depleted (<10 ppb), as observed
203 previously.[9,16] Both Polluted and Not Polluted periods experienced nearly the same levels of O_3,
204 on average, during the campaign, showing that the levels of NO_x, rather than O_3 were likely
205 responsible for the differences in Cl_2 mole ratios observed.

206

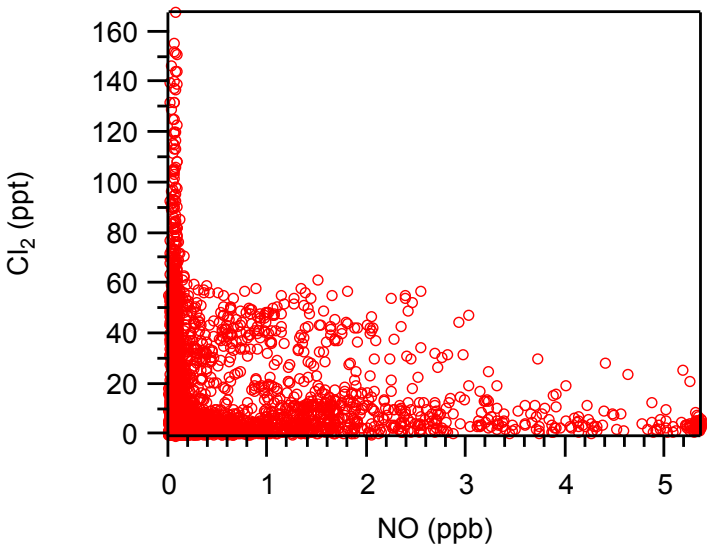

Figure S10: 1 min averaged Cl_2 observations versus 1 min averaged NO observations (R^2 = 0.004) during PHOXMELT. Note that the NO instrument LOD is 0.4 ppb.

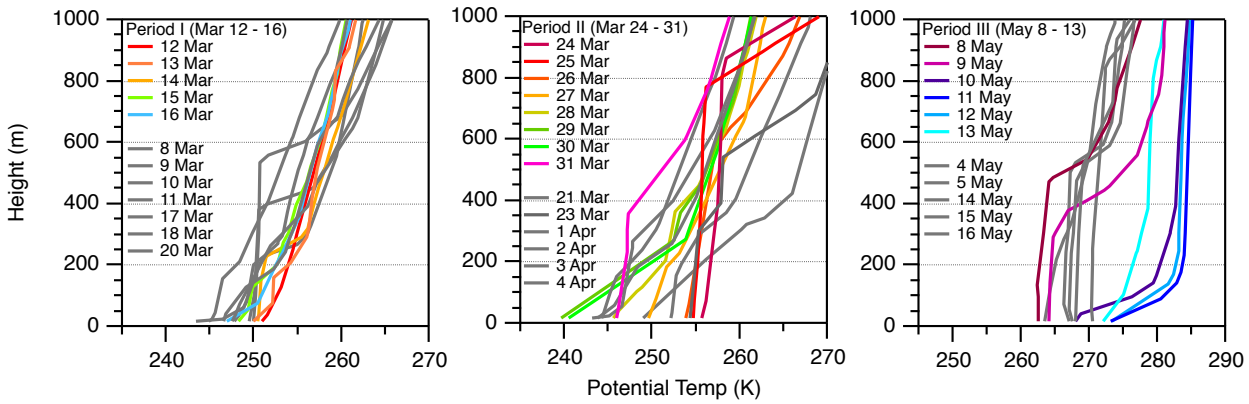

Figure S11: Vertical potential temperature measurements from daily soundings at the PABR station in Utqiaġvik. All times are 12:00 UTC (03:00 AKST). Soundings from the three polluted periods are shown with colored traces, and soundings from the surrounding days are shown with gray traces. All data are available at http://weather.uwyo.edu/upperair/sounding.html.

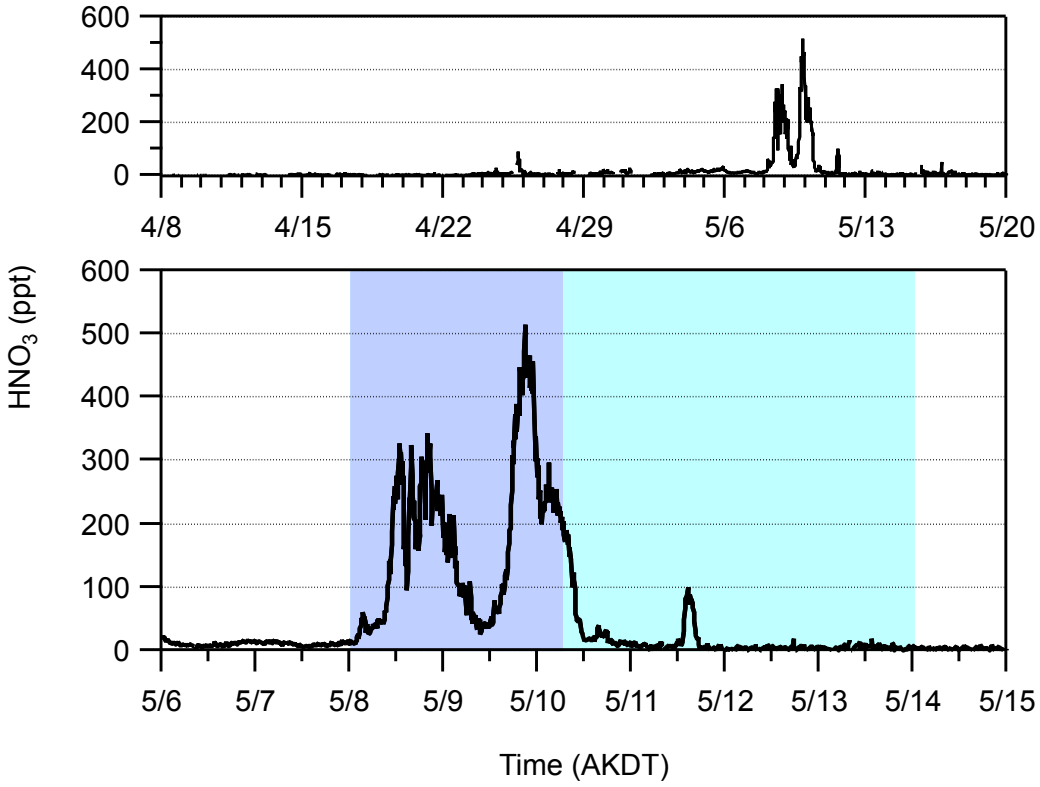

215

216 **Figure S12:** 10 min averaged mole ratios of HNO_3 during (*top panel*) April 8 – May 20 and
217 (*bottom panel*) Period III (blue shading), including the period influenced by the North Slope of
218 Alaska oilfields (purple shading). The HNO_3 removal efficiency of the glass wool scrubber during
219 backgrounds was 40-60%; therefore, the HNO_3 mole ratios shown are an underestimate.

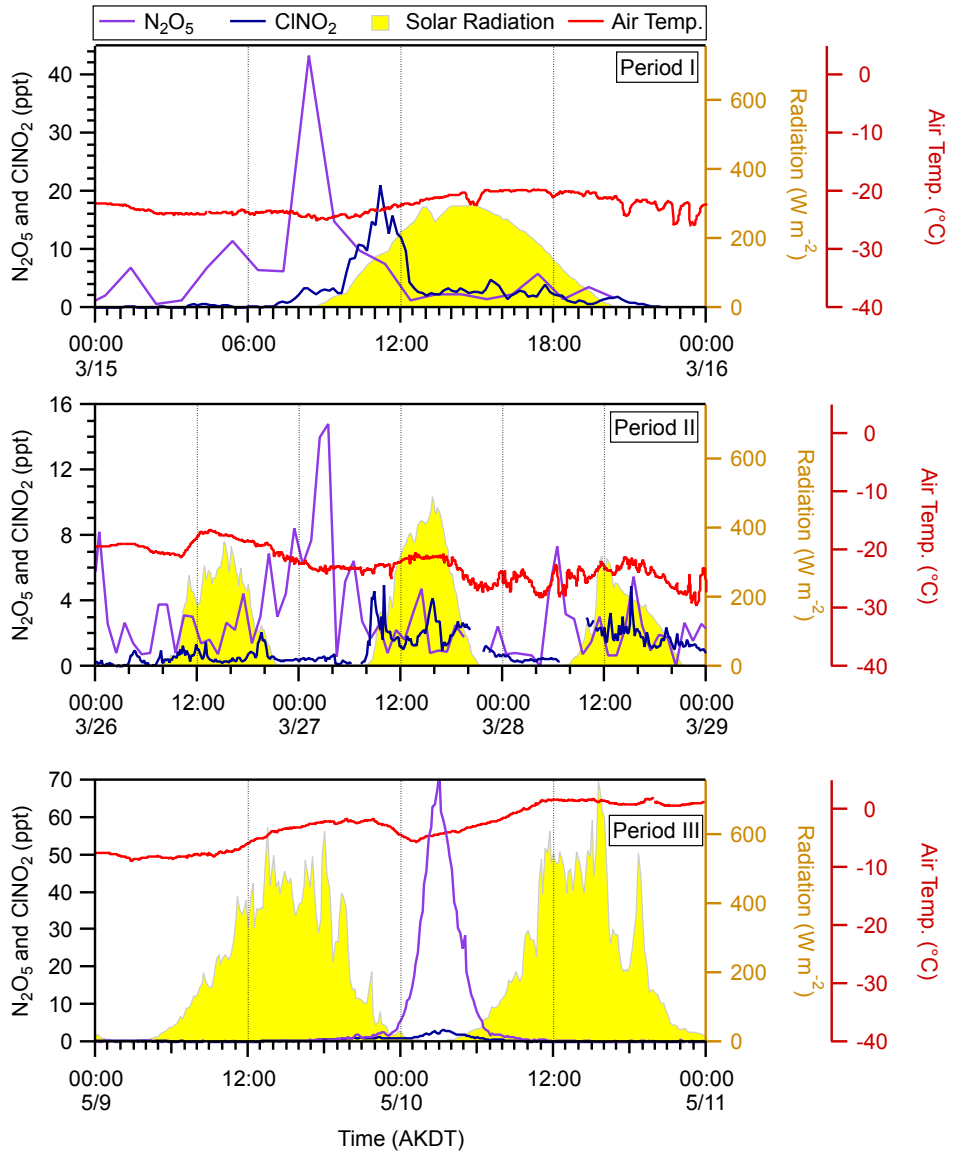

220

221 **Figure S13:** Mole ratios of N_2O_5 and $ClNO_2$ during Period I (*top panel*), Period II (*middle panel*)
222 and Period III (*bottom panel*), shown with measurements of solar radiation and air temperature.
223 All $ClNO_2$ mole ratios were 10 min averaged, and N_2O_5 mole ratios were hourly mass scans for
224 Periods I and II and 10 min averaged for Period III.

225

226

References

(1) Hönninger, G.; von Friedeburg, C.; Platt, U. Multi Axis Differential Optical Absorption Spectroscopy (MAX-DOAS). *Atmos. Chem. Phys.* **2004**, *4* (1), 231–254.

(2) Peterson, P. K.; Simpson, W. R.; Pratt, K. A.; Shepson, P. B.; Frieß, U.; Zielcke, J.; Platt, U.; Walsh, S. J.; Nghiem, S. V. Dependence of the Vertical Distribution of Bromine Monoxide in the Lower Troposphere on Meteorological Factors Such as Wind Speed and Stability. *Atmos. Chem. Phys.* **2015**, *15* (4), 2119–2137.

(3) Simpson, W. R.; Peterson, P. K.; Frieß, U.; Sihler, H.; Lampel, J.; Platt, U.; Moore, C.; Pratt, K. A.; Shepson, P. B.; Halfacre, J.; Nghiem, S. V. Horizontal and Vertical Structure of Reactive Bromine Events Probed by Bromine Monoxide MAX-DOAS. *Atmos. Chem. Phys.* **2017**, *17* (15), 9291–9309.

(4) Liao, J.; Sihler, H.; Huey, L. G.; Neuman, J. A.; Tanner, D. J.; Friess, U.; Platt, U.; Flocke, F. M.; Orlando, J. J.; Shepson, P. B.; Beine, H. J.; Weinheimer, A. J.; Sjostedt, S. J.; Nowak, J. B.; Knapp, D. J.; Staebler, R. M.; Zheng, W.; Sander, R.; Hall, S. R.; Ullmann, K. A Comparison of Arctic BrO Measurements by Chemical Ionization Mass Spectrometry and Long Path-Differential Optical Absorption Spectroscopy. *J. Geophys. Res.* **2011**, *116*, D00R02.

(5) Thaler, R. D.; Mielke, L. H.; Osthoff, H. D. Quantification of Nitryl Chloride at Part per Trillion Mixing Ratios by Thermal Dissociation Cavity Ring-down Spectroscopy. *Anal. Chem.* **2011**, *83*, 2761–2766.

(6) Sjostedt, S. J.; Huey, L. G.; Tanner, D. J.; Peischl, J.; Chen, G.; Dibb, J. E.; Lefer, B.; Hutterli, M. A.; Beyersdorf, A. J.; Blake, N. J.; Blake, D. R.; Sueper, D.; Ryerson, T. B.; Burkhart, J.; Stohl, A. Observations of Hydroxyl and the Sum of Peroxy Radicals at Summit, Greenland during Summer 2003. *Atmos. Environ.* **2007**, *41* (24), 5122–5137.

(7) Pollack, I. B.; Lerner, B. M.; Ryerson, T. B. Evaluation of Ultraviolet Light-Emitting Diodes for Detection of Atmospheric NO2by Photolysis - Chemiluminescence. *J. Atmos. Chem.* **2010**, *65* (2–3), 111–125.

(8) Bertram, T. H.; Thornton, J. A.; Riedel, T. P. An Experimental Technique for the Direct Measurement of N2O5 Reactivity on Ambient Particles. *Atmos. Meas. Tech.* **2009**, *2*, 231–242.

(9) Custard, K. D.; Pratt, K. A.; Wang, S.; Shepson, P. B. Constraints on Arctic Atmospheric Chlorine Production through Measurements and Simulations of Cl2 and ClO. *Environ. Sci. Technol.* **2016**, *50* (22), 12394–12400.

(10) Huff, A. K.; Abbatt, J. P. D. Gas-Phase Br2 Production in Heterogeneous Reactions of Cl2, HOCl, and BrCl with Halide-Ice Surfaces. *J. Phys. Chem. A* **2000**, *104* (31), 7284–7293.

(11) Appelman, E. H.; Gosztola, D. J. Aqueous Peroxynitric Acid (HOONO2): A Novel Synthesis and Some Chemical and Spectroscopic Properties. *Inorg. Chem.* **1995**, *34* (4), 787–791.

(12) Bollinger, M. J.; Sievers, R. E.; Fahey, D. W.; Fehsenfeld, F. C. Conversion of Nitrogen Dioxide, Nitric Acid, and n-Propyl Nitrate to Nitric Oxide by Gold-Catalyzed Reduction with Carbon Monoxide. *Anal. Chem.* **1983**, *55* (12), 1980–1986.

(13) Ridley, B. A.; Grahek, F. E. A Small, Low Flow, High Sensitivity Reaction Vessel for NO Chemiluminescence Detectors. *J. Atmos. Ocean. Technol.* **1990**, *7* (2), 307–311.

(14) Day, D. A.; Wooldridge, P. J.; Dillon, M. B.; Thornton, J. A.; Cohen, R. C. A Thermal

Dissociation Laser-Induced Fluorescence Instrument for in Situ Detection of NO2, Peroxy Nitrates, Alkyl Nitrates, and HNO3. *J. Geophys. Res. Atmos.* **2002**, *107* (D6), 4046.

(15) Kolesar, K. R.; Cellini, J.; Peterson, P. K.; Jefferson, A.; Tuch, T.; Birmili, W.; Wiedensohler, A.; Pratt, K. A. Effect of Prudhoe Bay Emissions on Atmospheric Aerosol Growth Events Observed in Utqiaġvik (Barrow), Alaska. *Atmos. Environ.* **2017**, *152*, 146–155.

(16) Liao, J.; Huey, L. G.; Liu, Z.; Tanner, D. J.; Cantrell, C. A.; Orlando, J. J.; Flocke, F. M.; Shepson, P. B.; Weinheimer, A. J.; Hall, S. R.; Ullmann, K.; Beine, H. J.; Wang, Y.; Ingall, E. D.; Stephens, C. R.; Hornbrook, R. S.; Apel, E. C.; Riemer, D. D.; Fried, A.; Mauldin, R. L.; Smith, J. N.; Staebler, R. M.; Neuman, J. A.; Nowak, J. B. High Levels of Molecular Chlorine in the Arctic Atmosphere. *Nat. Geosci.* **2014**, *7* (2), 91–94.